Desalination and Water Treatment
www.deswater.com

doi: 10.5004/dwt.2018.21851

108 (2018) 223–234
March

Influence of the activation method of agro-industrial wastes in the removal of lead

Marianela Gimenez[a,*], Fabiana Sardella[a], Cristina Deiana[a], Karim Sapag[b]

[a]*Instituto de Ingeniería Química, Facultad de Ingeniería, Universidad Nacional de San Juan, CONICET, Avenida Libertador 1109 Oeste, San Juan 5400, Argentina, Tel. +54-264-4211700 Ext. 453/32; emails: mgimenez@unsj.edu.ar (M. Gimenez), mfs@unsj.edu.ar (F. Sardella), acdeiana@unsj.edu.ar (C. Deiana)*
[b]*INFAP-CONICET, Universidad Nacional de San Luis, Avenida Ejército de los Andes 950, San Luis 5700, Argentina, email: ksapag@unsl.edu.ar*

Received 12 May 2017; Accepted 23 December 2017

ABSTRACT

The adsorption on activated carbon has been shown to be very effective for the removal of heavy metals from water. This work details the removal of lead by adsorption onto activated carbon obtained from wastes of grape industrialization, in batch and column operation, under different conditions in order to correlate the adsorbents properties with their performance. Activated carbons, obtained from grape lex and grape stalk by physical and chemical activation, were characterized by Brunauer, Emmet and Teller (BET) surface area, pore volumes, point of zero charge pH and surface functional groups through Boehm method, Fourier transform infrared spectroscopy and temperature programmed decomposition. The results showed better textural properties for the adsorbents obtained by chemical activation, whose BET areas were 978 and 1,217 $m^2 g^{-1}$. Chemical characterization also showed a marked difference between both activation routes, yielding carbons with a marked basic character by physical activation and acid by the other way. Due to their dissimilar textural and chemical properties, all products exhibited different performance in batch and continuous assays. The maximum adsorption capacity was 49.95 mg g^{-1}, achieved at a bed height of 15 cm and a feed concentration of 100 mg L^{-1} using steam activated grape lex briquettes as adsorbent.

Keywords: Agro-industrial wastes; Activated carbon; Activation methods; Lead; Adsorption

1. Introduction

In recent years, the legislation of the countries on environmental quality set stricter regulations on the treatment and disposal of wastes, leading the industry to increase investments in research with a focus on the treatment and reutilization of its liquid and solid effluents.

Adsorption onto activated carbon has been found to be superior to other wastewater treatment techniques because of its capability for removing a broad range of different kind of adsorbates efficiently, and its simplicity of design [1]. Heavy metals such as cobalt, lead, copper, nickel, chromium and zinc are found among the most toxic pollutants detected in waste streams, from mining operations, tanneries, electronics, electroplating, petrochemical and textile industries. It is well known that these elements bioaccumulate in living tissues causing health disorders because of their disruptive integration into normal biochemical processes [2].

Activated carbons are usually obtained from materials with high carbon content and possess a great adsorption capacity, which is mainly determined by their porous structure [3]. The inherent nature of the precursor or starting material, as well as the method and conditions employed for carbon synthesis, strongly affects the final pore size distribution and the adsorption properties of the activated carbons [4]. Lignocellulosic materials constitute the more

* Corresponding author.

commonly used precursors; around 45 wt% of the total raw materials used for the manufacture of activated carbons. Low contents of inorganic materials are desirable in the preparation of activated carbons with low ash content, but relatively high volatile content is also needed to control carbon porosity. Both characteristics are common to most of the lignocellulosic materials used for the production of activated carbons [5]. Thus, the use of agro-industrial waste as cheap precursors of activated carbon is an interesting alternative to add value to this residue and, at the same time, solve the problems related to its final disposal [6–9].

Grape stalk is the woody fraction of the cluster and is the waste left after the fruit industrialization [10]. Grape lex is the solid residue resulting from the grape oil extraction process. Neither of these materials is commercially exploded nowadays, causing important loses to the industries that must dispose them.

The adsorption equilibrium and kinetics for each specific contaminant are related to the chemical surface and the porous structure of the activated carbon used as adsorbent. To evaluate activated carbons performance, it is critical to develop models and experimental procedures that could accurately describe the dynamics of the pollutant adsorption and desorption under a variety of operating conditions [11].

This work presents complementary results of previous studies carried out to obtain complete information about the behavior of grape stalk and lex to prepare activated carbons and its application for lead removal. These studies are very important for producers of this region (San Juan and Mendoza Provinces), because the principal economic activity is the viticulture and the disposal of wastes produced is a permanent preoccupation. For example, about 100 million kilograms of stalks are generated annually in grape industrialization to produce wines and musts. On the other hand, pollution of waterways by toxic metals is of concern in the region because of the intense mining–metallurgy activity developed in recent years, and lead is one of the elements generally present in the mineral exploited.

In this paper, activated carbons obtained from grape lex and grape stalk by physical and chemical activation were characterized and used under different operation conditions in order to correlate the adsorbents properties with their performance. Kinetic, equilibrium and fixed-bed column lead adsorption studies were analyzed and related to the adsorbents activation method.

2. Experimental methods

Two residual biomasses were used as raw materials to obtain the adsorbents: grape stalk and grape lex.

The residues were sieved and the fraction retained by a 12 mesh ASTM sieve was collected for the assays. The material was dried in an oven at 383 K for 24 h. Each sample was separated into two fractions; the first one was subjected to chemical activation and the other one to physical activation.

2.1. Preparation of adsorbents

Chemical activation was performed using phosphoric acid as activating agent. One of the most important variables of this activation method is the impregnation ratio, defined as the ratio between the mass of the chemical agent used for activation and the mass of precursor. Based on previous studies, an impregnation ratio (mass of P/mass of carbonaceous material) of 0.39 g g^{-1} was adopted [10]. Samples were impregnated with phosphoric acid (85% w/w) and kept in contact with the reagent in an oven at 303 K for 17 h then the temperature was raised to 383 K and maintained for 24 h to dry the material. The dried samples were placed in a sealed stainless steel reactor and subjected to a heat treatment at high temperature in a muffle furnace in the absence of oxygen, for 1 h at 773 K. The product was washed with distilled water, in a batch reactor with a solid to liquid ratio of 1:2 and contact time of 1 h. This step was repeated until final pH reached distilled water pH. Then, it was dried in an oven for 24 h.

For physical activation, the wastes, as received, were heated in an inert atmosphere at a rate of 1.4 K min^{-1}, from room temperature up to 773 K and kept at that temperature for 2 h. This step was carried out in a stainless steel carbonization reactor electrically heated. Carbonized grape stalk was subjected to a leaching step with hydrochloric acid (5% w/w) at room temperature to reduce its alkaline metal content [10].

Carbonized materials and those carbonized and leached were briquetted using grape must as binder. The briquettes were made by mixing in a mortar measured amounts of char and binder in a ratio of 4:1. The resulting mixture (1 g) was submitted to pressures of 140 MPa for 6 min, into a 10 mm into a 10 mm inner diameter cylindrical stainless steel mould held in a hydraulic press.

Briquettes were activated, using steam as activating agent, in a stainless steel tubular reactor (30 mm internal diameter and 300 mm length), heated in an electric furnace with automatic temperature control. The heating step, from room to activation temperatures, was carried out in flowing nitrogen gas at 288 K min^{-1}. In all assays, the reactor was loaded with 15 g of briquettes, which were submitted to a steam flow of 1.7 g (g char)$^{-1}$ (h)$^{-1}$ for 105 min. Activated briquettes were measured, weighed and stored.

The adsorbents obtained by physical activation were named PS and PL, for grape stalk and grape lex, respectively, and the ones obtained by chemical activation were CS and CL for the same materials.

2.2. Characterization of raw materials and activated carbons

Elemental analysis of the raw materials was carried out in a Carlo Erba EA1108 CHNSO equipment, and proximate analysis (moisture, ash, volatile matter and fixed carbon) was performed by following ASTM standards [12–14]. For the lasts, a muffle oven and a furnace were used.

In order to evaluate the textural properties of the materials, adsorption–desorption isotherms of nitrogen at 77 K were carried out in a Micromeritics, ASAP 2000 Model equipment. The specific surface area was calculated by the Brunauer, Emmet and Teller (BET) method, the total pore volume by the Gurvich rule at a relative pressure of p/p_0 = 0.98 and the micropore volume was obtained using the *t* plot method.

The point of zero charge pH (pH_{pzc}) was measured by following the method proposed by Noh and Schwartz [15]. Three aqueous solutions of different initial pH were prepared from a 0.01 M $NaNO_3$, using 0.01 M NaOH and 0.01 M

HNO_3 for its regulation. Different masses of each adsorbent under study were contacted in vials with 20 mL of each solution of sodium nitrate prepared at different initial pH. The equilibrium pH was measured after 4 d in contact at room temperature.

Basic and acid surface functional groups were determined by titration with hydrochloric acid and sodium hydroxide, respectively. Samples of 200 mg from each adsorbent were contacted with 20 mL of 0.05 N acid and basic solution in flasks that were sealed and maintained under stirring for 48 h at room temperature. Suspensions were separated by centrifugation and the final concentration of the solutions was determined by titration with NaOH and HCl.

Surface functional groups were also studied by Fourier transform infrared (FTIR) spectroscopy, which were obtained using a Nicolet 380 equipment. Pressed potassium bromide (KBr) pellets at a sample/KBr weight ratio of 1:100 were scanned and recorded between 4,000 and 400 cm^{-1}. The samples were previously placed in an oven at 330 K for 72 h to remove any water, if present.

Temperature-programmed decomposition (TPD) profiles were obtained with a Quantachrome Analyzer 3000 CHEMBET with thermal conductivity detector. A 10 mg sample was heated under He atmosphere, 20 cm^3 min^{-1}, at a rate of 5 K min^{-1}, from room temperature to 1,273 K. The evolution of CO_2 and CO was monitored by mass spectrometry using a Quadropole Analyzer Smart-IQ VG + Gas.

The morphological characteristics of the activated carbons surface were investigated by scanning electron microscopy (SEM) in a JEOL JSM-6610LV (MEB) equipment. Samples were sputter coated with Au prior to the scanning.

2.3. Lead adsorption assays

In order to evaluate the adsorbent properties of activated carbons, kinetic, batch and continuous assays were performed. For these tests, $Pb(NO_3)_2$ solutions were prepared using deionized water.

Lead kinetic adsorption assays were performed to obtain the minimum contact time. Adsorbent samples of 30 mg were placed in sealed flasks with 50 mL of a 100 and 25 mg L^{-1} solution of Pb^{2+}. The suspensions were stirred at 120 rpm in a thermostatic bath at 293 K, varying the contact time for each flask. The experiments were carried out at a pH value of 5.5 ± 0.2, which is the optimum value for this system [16]. From these assays the minimum contact time necessary to reach adsorption equilibrium was obtained.

Two kinetic models, the pseudo-first-order [17] and pseudo-second-order [18] were selected in this study to describe the adsorption process. The linear equations of both models are shown by Eqs. (1) and (2), respectively:

$$\ln(q_e - q_t) = \ln q_e - k_1 t \tag{1}$$

$$\frac{t}{q_t} = \frac{1}{k_2 q_e^2} + \frac{1}{q_e} t \tag{2}$$

where q_e and q_t are the quantities (mg g^{-1}) adsorbed per unit mass of adsorbent at equilibrium and at a time t (min), respectively, k_1 (min^{-1}) and k_2 (g mg^{-1} min^{-1}) are the rate constants of pseudo-first-order and pseudo-second-order kinetics.

Batch assays were performed to obtain adsorption isotherms. Masses of 30 mg of each adsorbent were contacted with 50 mL of $Pb(NO_3)_2$ solutions at several concentrations (30, 45, 60, 75, 90, 100 and 120 mg L^{-1}) and shaken at 120 rpm in a thermostatic bath at 293 K for the minimum contact time. Once equilibrium time was reached, samples were centrifuged, and the metal concentration was determined in the liquid phase by atomic absorption spectrometry (AAS). The pH for all adsorption tests was adjusted to 5.5 ± 0.2.

Lead uptake (q) was calculated from the mass balance as follows:

$$q = V\left(\frac{C_0 - C_f}{M}\right) \tag{3}$$

where V is the solution volume (L) and M is the weight of activated carbon (g) used. C_0 and C_f are the initial and final Pb^{2+}concentrations (mg L^{-1}), respectively.

The Freundlich and Langmuir isotherms were used to describe lead adsorption from bulk solution onto activated carbon briquettes, assuming no interaction among adsorbed molecules.

The Freundlich isotherm is expressed as follows [19]:

$$q = KC_e^{\frac{1}{n}} \tag{4}$$

where q is the amount of metal adsorbed per unit weight of adsorbent (mg g^{-1}) and C_e is the equilibrium concentration of the adsorbate (mg L^{-1}). K and n are the model constants related to the adsorption capacity of the solid and the intensity of adsorption, respectively.

The Langmuir isotherm is expressed as [20]:

$$q = \frac{Q_o b C_e}{1 + bC_e} \tag{5}$$

where Q_o is the monolayer adsorption capacity (mg g^{-1}) and b is the Langmuir constant (L mg^{-1}).

Continuous tests were carried out in a glass column of 14 mm inner diameter and 250 mm length, supplemented with a cooling jacket. The adsorbent was crushed and sieved to obtain a grain size between 0.7 and 1.8 mm and packed in the column in a 150 mm bed. In these tests the mass of adsorbent (g) to solution flow rate (mL/min) ratio was kept 2:1 and the temperature at 293 K. The column was operated in an upflow mode. Metal solution initial concentrations were 100 and 25 mg L^{-1}, with initial pH adjusted to the predetermined optimum value. To analyze the behavior of this variable, the pH was measured in the column effluent solutions throughout the course of each trial.

After continuous adsorption tests were finished, desorption assays were carried out using HNO_3 0.5 M as eluent. These experiments were developed in the same operating conditions of the continuous adsorption tests.

From the experimental data breakthrough curves were constructed and adjusted to Thomas and dose response model.

The expression of Thomas model is given by [21]:

$$\frac{C_t}{C_0} = \frac{1}{\left[1+\exp\left(k/Q\right)\left(q_m - C_0 Q t\right)\right]} \tag{6}$$

The modified dose response model can be written as [22]:

$$\frac{C_t}{C_0} = 1 - \frac{1}{1+\left(\frac{C_0 Q t}{q_m}\right)^a} \tag{7}$$

where C_0 and C_t are the influent and effluent concentrations (mg L^{-1}) respectively, k is the Thomas rate constant (L mg^{-1} min^{-1}), q is the maximum adsorption capacity (mg g^{-1}), m is the mass of adsorbent in the column (g), Q is the feed flow (mL min^{-1}), t is the time (min) and a is the dose response model parameter.

Metal concentration was determined by AAS, in a Perkin ElmerAA-100, with hollow cathode lamp.

Batch and continuous assays were performed by duplicate and the average value was informed.

3. Results and discussion

Table 1 presents the results of proximate and elemental analysis of the raw materials studied. Grape stalk showed an outstanding high ash content which led to the addition of a leaching step before physical activation [10]. Grape lex showed a high fix carbon value, which is a relevant condition in raw materials for activated carbons production.

Table 2 presents results of the textural and chemical characterization of the adsorbents. Even though chemical activation produced higher surface areas, the activated carbons obtained presented values in the range reported for similar materials. Specific BET surface area for activated carbon prepared from oil palm fiber with 715.6 m^2 g^{-1} was informed by Nwabanne and Igbokwe [4], coconut pith and fiber with 505 and 1,034 m^2 g^{-1}, respectively, were reported by Johari et al. [23]. All adsorbents showed similar micropore volume, but chemically activated carbons presented a higher mesopore to total pore volume ratio, 0.74 for CS and 0.57 for CL. In physically activated carbons, mesopore contribution represented less than 0.35 of total pore volume.

Fig. 1 shows the SEM images of the activated carbons from grape stalk and grape lex. Images (a) and (b) correspond to the adsorbents prepared by the physical method. It can be seen that the stalk activated carbon maintains the fibrous structure of the original material, although this material was finely ground to prepare briquettes. In opposition, the lex activated carbon presents a uniform aspect, also observed in its precursor. These carbons present particles with a smooth aspect, randomly distributed, which could be attributed to the grape must used as binder in the briquettes. The adsorbents prepared by the chemical method also show structural differences (Figs. 1(c) and (d)), but in both materials the surfaces are more softened compared with adsorbents obtained by the physical route. This could be related to the differences in the aggressiveness of the activating agents.

In relation to surface chemistry it can be observed that chemically activated carbons presented lower pH_{pzc} values, which were near to the ones obtained for raw materials [16]. Physically activated carbons showed pH_{pzc} markedly high, which rise throughout the activation process (carbonization and activation with steam). It is noteworthy mentioning that the adsorption of contaminates from liquids solutions depends on the adsorbate–adsorbent system pH. In metal adsorption, this parameter is even more important because of the influence on its speciation. As mentioned before, the best pH for lead adsorption was in the range 5.5–6. These values are over the pH_{pzc} of the chemically activated carbons, which leads to negatively charged surfaces that would favor electrostatic attraction between the surface and the metal ions.

Table 1
Characterization of raw materials

Material	Proximate analysis (%)				Elemental analysis (db)[a] (%)				pH_{pzc}
	Moisture	Ash	Volatile matter	Fix carbon	N	C	H	S	
Grape stalk	20.2	12.5	53.5	13.9	0.37	46.14	5.74	0	4.59
Grape lex	19.3	5.6	44.4	30.7	2.91	52.27	5.38	0	4.25

[a]db, Dry basis.

Table 2
Characterization of adsorbents

Material	BET area (m^2 g^{-1})	V_T (m^3 g^{-1})	$V\mu$ (m^3 g^{-1})	V_m (m^3 g^{-1})	pH_{pzc}	Total acid groups (meg g^{-1})	Total basic groups (meg g^{-1})
PS	723	0.37	0.25	0.12	10.02	1.80	0.27
PL	795	0.40	0.27	0.13	12.03	1.35	0.27
CS	968	0.94	0.25	0.69	4.43	2.54	1.66
CL	1,217	0.75	0.32	0.43	3.68	1.44	1.40

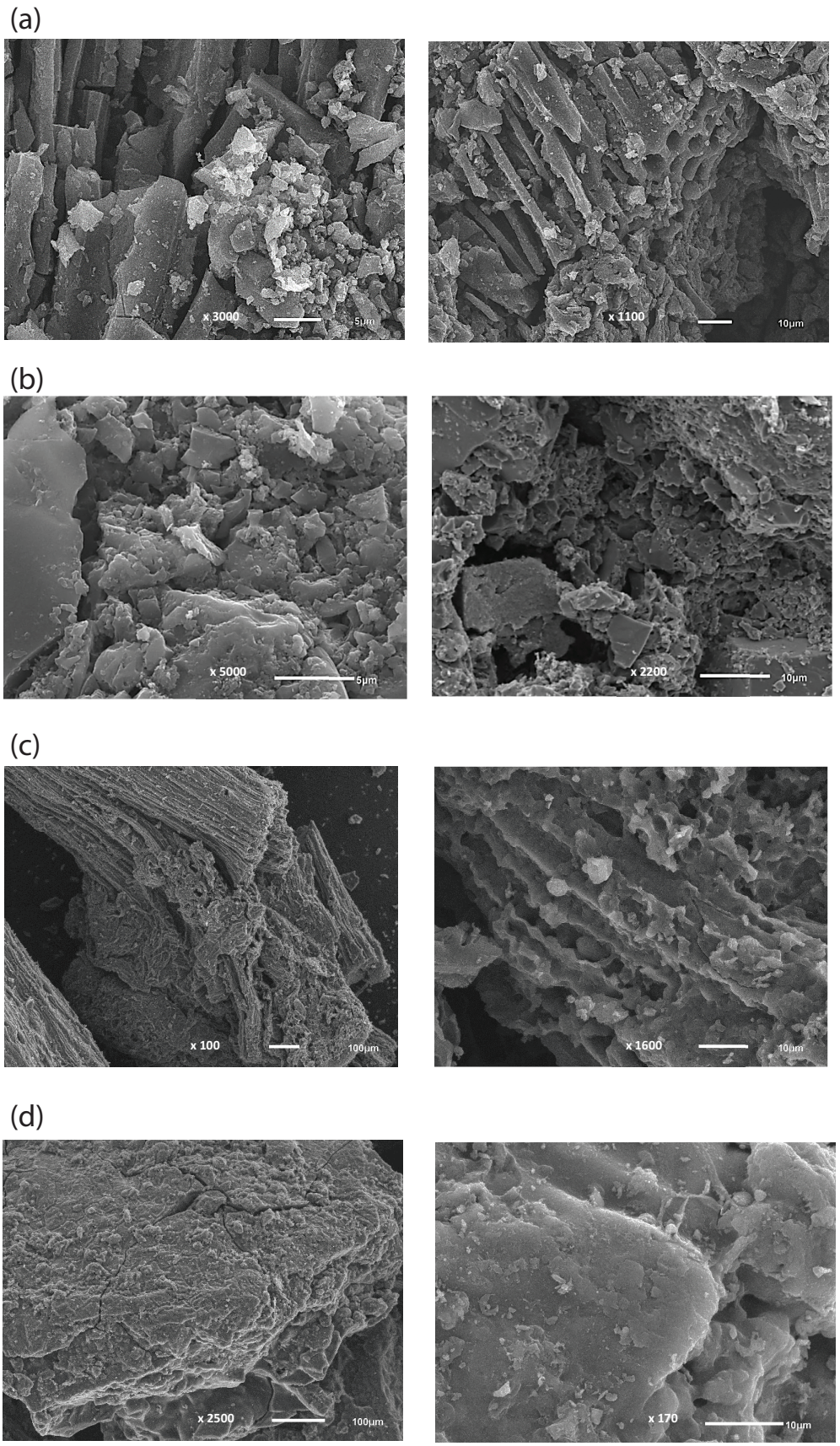

Fig. 1. SEM images of PS (a), PL (b), CS (c) and CL (d) adsorbents.

Surface functional groups affect activated carbons acidic/basic character conditioning its hydrophobic/hydrophilic behavior and, consequently, many of its applications. The characterization of the surface chemistry in this kind of adsorbent is not easy to perform and it is common to use two or more techniques that provide complementary information. Boehm titration, FTIR spectroscopy and TPD are widely accepted techniques for this purpose and they provide information about the kind and intensities of the surface functionalities.

TPD was used for the characterization of surface oxides present in the adsorbents. Oxygen containing groups decompose upon heating, evolving CO_2 and CO at different temperatures. Fig. 2 presents CO_2 and CO profiles for the activated carbons from grape stalk and lex. CO_2 evolution between 373 and 723 K, related to carboxylic groups, is higher for CS sample, followed by the physically activated carbons and CL sample with the lowest signal, representing the least amount of this group. The peak around 973 K, attributable to lactone groups, was higher in PL sample, followed by CS and with the lowest intensity CL and PS samples. The presence of anhydrides is evidenced by the evolution of CO and CO_2 in a temperature range between 673 and 923 K, with higher peaks for CS, CL, PS and PL, respectively. Phenols decomposition to CO at temperatures between 773 and 973 K is observed in CS, CL, PS and PL, named in increasing order of concentration of this group. CO profiles of the chemically activated adsorbents exhibited a peak around 973 K that may be assigned to ether groups, present in greater amounts in CL. The evolution of CO at high temperatures, between 1,023 and 1,273 K, is attributed to carbonyl and quinones, and was observed in CL, PL and PS samples [24,25].

Fig. 3 shows the FTIR spectra of activated carbon samples, CS, CL, PS and PL. All the samples showed the same absorption bands at the same wavenumbers, indicating that the functional groups present were very similar. Low intensity bands at 900 cm^{-1}, attributed to aromatic C–H bonds, were observed in all samples [26]. This signal was observed with higher intensity in CS, PL and PS. A band in the region of 1,050cm^{-1} was observed and it was attributed to the stretching vibrations of the C–O bonds of esters, alcohols, phenols or ethers [27]. Bands in the ranges of 1,160–1,370 and 1,675–1,790 cm^{-1} indicated the presence of lactone groups. Quinone groups, reflected in the C–O band between 1,550 and 1,680 cm^{-1}, and carboxylic acids, with bands in the ranges of 1,120–1,200, 1,665–1,760 and 2,500–3,300 cm^{-1}, were observed in all samples with varied intensity [28]. A wide absorption band between 3,600 and 3,200 cm^{-1}, with a maximum at 3,420 cm^{-1}, attributed to hydroxyl groups and chemisorbed water, also appears in all samples. The position of the band is characteristic of stretching vibrations of hydroxyl compounds, while the amplitude indicates high degrees of association due to hydrogen bonds [29]. Thus, it is estimated that the adsorbents studied contain hydroxyl groups from carboxyl, phenol and alcohol.

FTIR spectra and TPD profiles showed that sample CS was the most functionalized material among the ones studied. These results are coincident with the total acid and basic group contents, determined by Boehm titration, for this material, presented in Table 2. It has been reported that oxygenated acid groups, such as the carboxylic, phenolic and lactonic, favor heavy metals adsorption [30]. Therefore, the

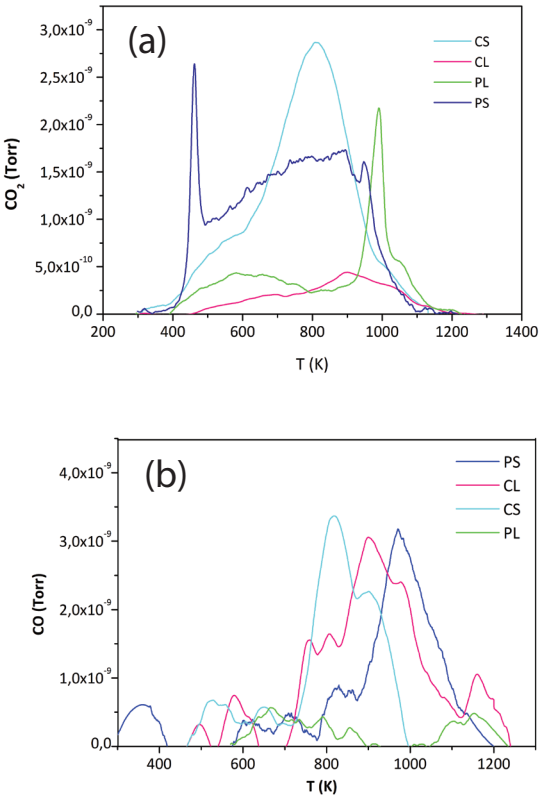

Fig. 2. TPD spectra of (a) CO_2 and (b) CO.

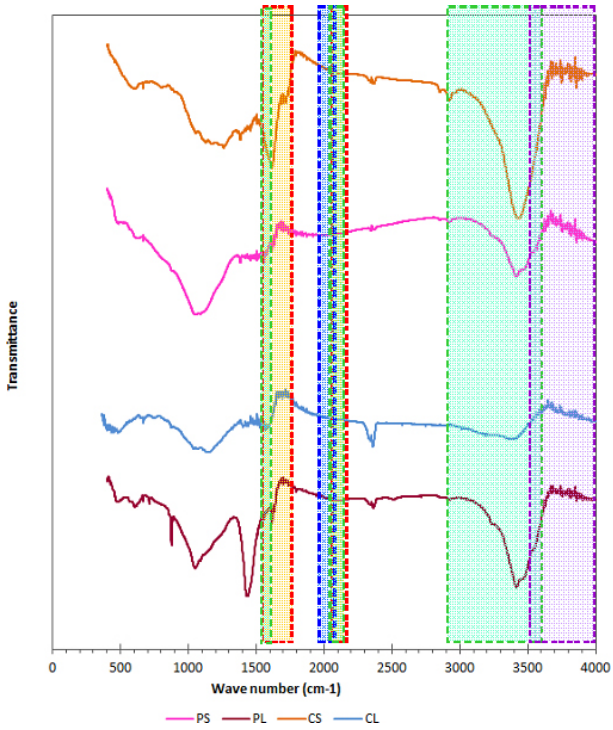

Fig. 3. FTIR spectra of activated carbons from grape stalk and lex.

presence of these groups in the activated carbons analyzed in this work would be favorable for the removal of the heavy metals studied, but this should be positively coupled with the textural properties and the operating conditions in the adsorption processes.

Fig. 4(a) presents the results of the kinetic assays for initial lead concentration of 100 mg L^{-1}. It can be observed that PL sample requires the highest contact time to reach adsorption equilibrium and removes only 58% of the metal initially present. The other adsorbents showed better performances with equilibrium times around 30 min and removal efficiencies over 70%. The results from kinetic assays performed at 25 mg L^{-1} evidenced adsorption capacities similar to the ones obtained at 100 mg L^{-1} (60%–65%), for chemically activated carbons. For physically activated carbons, the removal efficiency reached 90% for an initial concentration of 25 mg L^{-1}. It was also observed that PL and PS samples reached equilibrium faster. This improvement in the removal efficiency for a lower solution concentration could be attributed to the higher microporosity of steam activated carbons. Decreasing the initial concentration of the metal decreases the resistance to mass transfer and consequently enhances the performance of these adsorbents.

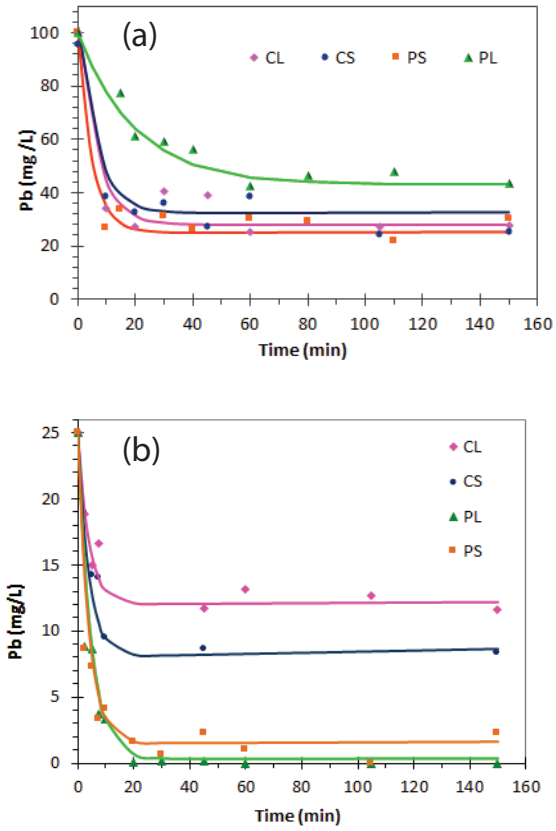

Fig. 4. Kinetic curve for lead adsorption at 100 mg L^{-1} (a) and 25 mg L^{-1} (b). Conditions: T = 293 K, pH = 5.5 and 120 rpm.

Kinetics models are frequently used to study the adsorption process. Pseudo-first-order, pseudo-second-order and intraparticle diffusion models are widely used for this purpose [31]. The first and second ones were used in this work to describe lead adsorption. Table 3 shows experimental model parameters and quantities retained at equilibrium ($q_{e,exp.}$) for different initial conditions.

Correlation coefficients (R^2) obtained for the pseudo-second-order model are greater than 0.974, showing a better fit to the experimental data than the first-order model (R^2 < 0.921). Experimental values of q_e are in good agreement with the theoretical values calculated by the pseudo-second-order model. This is not so with the ones calculated by the pseudo-first-order model. Therefore, the pseudo-second-order model is the one that best describes the kinetics for all adsorbate–adsorbent systems studied.

An analysis of values reported in Table 3 also reveals k_2 decreases with the increase of the initial metal concentration, which means that a longer time is needed to reach equilibrium at a higher concentration.

Wu et al. [32] defined the second-order rate index, k_2q_e, and proposed this index as a suitable parameter to describe adsorption kinetics. In this study, the k_2q_e values follow the order of PL < CS < CL < PS for an initial concentration of 100 mg L^{-1} and CL < CS < PS < PL at 25 mg L^{-1} (Table 3). As the k_2q_e value is the inverse of the half-life of adsorption process, the adsorption kinetics gets faster in this order, which is consistent with the experimental observations.

Table 3
Parameters of the pseudo-first-order and pseudo-second-order kinetic models for lead adsorption

		PS		PL		CS		CL	
	C_0 (mg L^{-1})	100	25	100	25	100	25	100	25
	$q_{e,exp.}$ (mg g^{-1})	125	38.3	95	42	125	28.3	121.7	23.3
Pseudo-first-order model	q_e (mg g^{-1})	15.6	8.1	99.7	12.99	38.5	7.4	29.98	12.8
	k_1 (min^{-1})	0.011	0.065	0.030	0.069	0.036	0.022	0.028	0.016
	R^2 (%)	92.1	83.0	84.1	90.2	72.0	66.6	74.6	79.5
Pseudo-second-order model	q_e (mg g^{-1})	125.0	41.8	97.1	42.2	147.1	28.4	123.5	22.2
	k_2 (g mg^{-1} min^{-1})	0.009	0.012	0.001	0.019	0.001	0.012	0.002	0.013
	R^2 (%)	99.3	99.9	98.9	99.9	97.4	99.9	99.5	99.6
	k_2q_e (min^{-1})	1.13	0.50	0.10	0.8	0.15	0.34	0.25	0.29

Adsorption isotherms of the four adsorbate–adsorbent systems, with the Langmuir and Freundlich fits, are summarized in Fig. 5.

It is apparent, the better performance of the chemically activated carbons, reaching removals that exceed 100 mg g^{-1} for both materials. In accordance with kinetic assays results, PL showed the lowest retention capacity. These results indicate that the porous development and the oxygen surface groups present in the adsorbent surfaces are combined favorably for metal retention.

Table 4 presents the parameters obtained for both models by non-linear regression, using Matlab R2010 software.

The regression coefficient (R^2) and the root mean square error (RMSE) were used to evaluate the fit of the models. The last one was calculated using Eq. (8):

$$\mathrm{RMSE} = \sqrt{\frac{\sum_{i=1}^{n}(X_{\mathrm{obs},i} - X_{\mathrm{model},i})^2}{N}} \tag{8}$$

where X_{obs} is the observed value, X_{model} is the value estimated by the model and N is the number of experimental points.

An analysis of Table 4 leads to the following observations. Lead isotherms for adsorbents obtained from grape stalk, samples PS and CS, were best adjusted by Freundlich model, with the highest values of the regression coefficient (R^2) and the smallest ones of RMSE. Instead, activated carbons produced from grape lex showed better fits to the Langmuir model. The chemically activated carbons exhibited higher retention capacities in relation to the steam activated samples, evidenced by the higher values of the parameters related to the adsorption capacity (q_{max}, K_F).

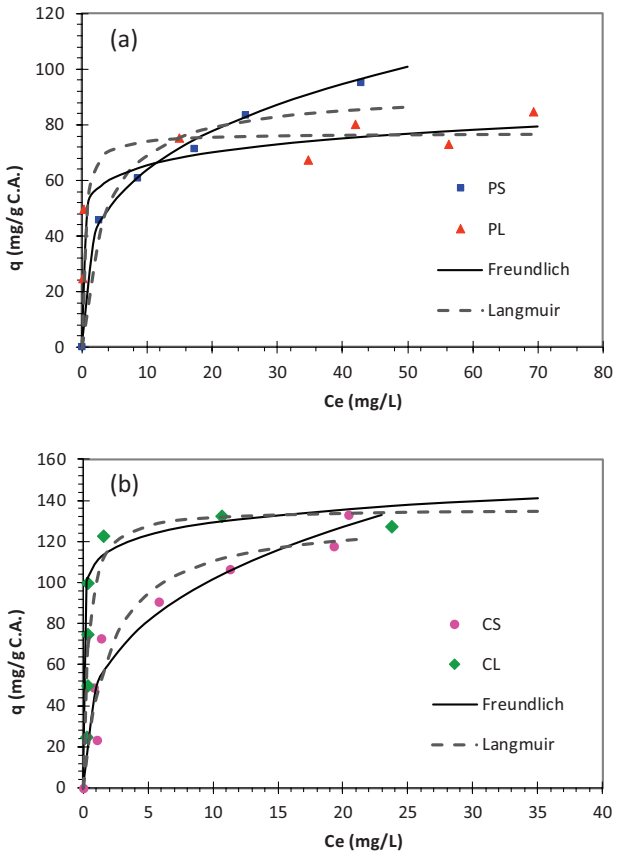

Fig. 5. Lead adsorption isotherms onto (a) physically activated carbons and (b) chemically activated carbons. The isotherms were fitted to the Langmuir (dotted lines) and Freundlich (continuous lines) models. Conditions: T = 293 K, pH = 5.5 and 120 rpm.

The essential characteristic of the Langmuir isotherm model can be described by the separation factor, R_L, represented by:

$$R_L = \frac{1}{1 + bC_0} \tag{9}$$

R_L values between 0 and 1 indicate that the adsorption is thermodynamically favorable [33]. For the studied lead-adsorbent systems, R_L took values between 0.003 and 0.3, in the concentration range 15–120 mg L^{-1}, indicating the adsorption process is favorable. For all adsorbate–adsorbent systems, Freundlich empirical factor values greater than unity were determined, indicating favorable lead adsorption conditions [34].

Continuous assays were conducted at two different initial concentrations. Breakthrough curves were obtained from these data. Breakthrough and exhaustion points were determined at C/C_0 0.10 and 0.90, respectively. The experimental curves, for PS and PL at a Pb^{2+} initial concentration of 100 mg L^{-1}, with the Thomas model and modified dose response model fit and effluent pH evolution profiles are presented in Fig. 6.

It can be seen that the pH profile has a sharp increase at the beginning of the assay, related to the markedly basic character of the physically activated carbons that lift these parameters, initially fixed at the optimum value. In accordance to lead speciation diagrams, insoluble species begin to appear at pH higher than 6 [35]. PL sample showed a better performance, which could be attributed to its higher pH_{pzc} value that maintained the solution pH at higher levels. In both cases lead removal was related with the confluence of adsorption and precipitation phenomena.

The influence of the activation method can be observed in Fig. 7, where the results of assays performed using lex activated by both methods are presented. As pH could not be controlled throughout the experiment, it showed different evolutions depending on the adsorbent characteristics.

Table 4
Freundlich and Langmuir model parameters

Model	Parameter	PS	PL	CS	CL
Freundlich	K_F ($mg^{1-(1/n)}$ $L^{1/n}$ g^{-1})	33.31	44.65	48.43	81.58
	$1/n$	0.28	0.14	0.32	0.19
	R^2	0.99	0.93	0.93	0.80
	RMSE	1.76	8.78	13.82	24.92
Langmuir	Q_o (mg g^{-1})	105.02	76.87	132.8	142.6
	b (L mg^{-1})	0.19	2.69	0.5	2.02
	R^2	0.95	0.95	0.92	0.91
	RMSE	7.34	7.24	14.82	15.84

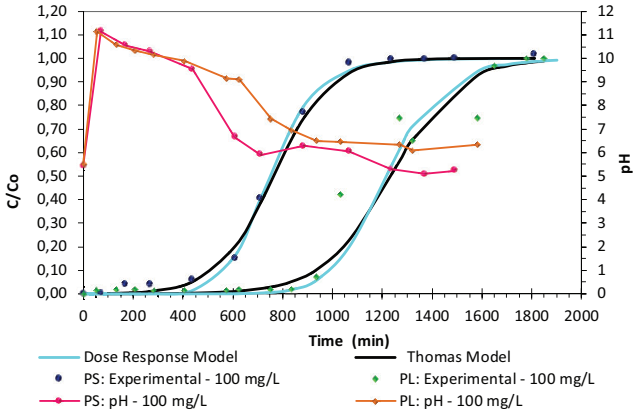

Fig. 6. Breakthrough curves for physically activated carbons at 100 mg L^{-1} fitted to mathematical models and pH profile. Conditions: bed height = 150 mm, T = 293 K and initial pH = 5.5.

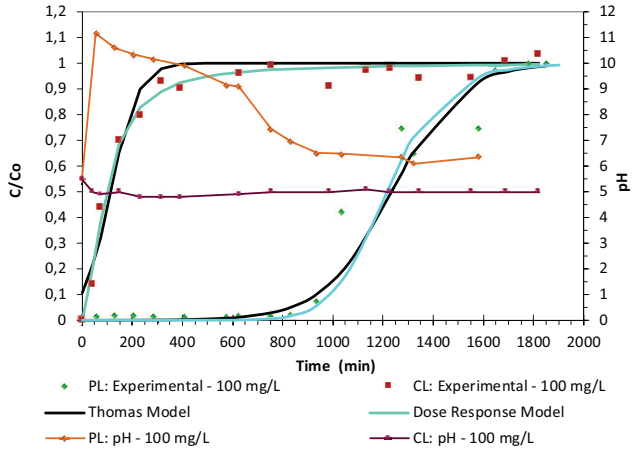

Fig. 7. Breakthrough curves for activated carbons obtained from lex grape at 100 mg L^{-1} fitted to mathematical models and pH profile. Conditions: bed height = 150 mm, T = 293 K and initial pH = 5.5.

Physically activated carbons, which pH_{pzc} is very high, caused the lift of pH values near 11 and the precipitation of lead insoluble species. This could indicate that initially lead removal has an important contribution of the precipitation phenomena, which disappears when pH decreases and adsorption becomes the main process.

When the chemically activated carbon CL, with a pH_{pzc} lower than 4, was used, the suspension pH stayed below the optimum. In this situation, protons compete against the metal ions for the adsorption sites leading to behavior different from that observed in equilibrium assays, where pH can be regulated at the optimum along the experiment.

The effect of initial solution concentration over adsorbents performance was studied. When lead concentrations increased from 25 to 100 mg L^{-1}, the breakthrough and the exhaustion time decreased for all the adsorbents. The adsorption process reached saturation faster and the breakthrough time appeared earlier with increasing influent lead concentration, probably due to the faster saturation of the activated

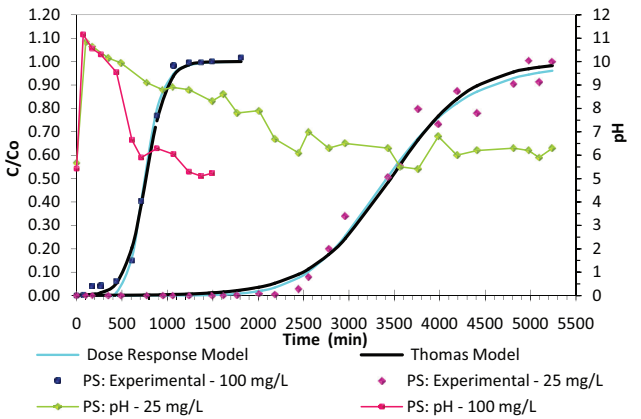

Fig. 8. pH profile and breakthrough curves for physically activated carbons obtained from stalk grape at 25 and 100 mg L^{-1}, fitted to mathematical models. Conditions: bed height = 150 mm, T = 293 K and initial pH = 5.5.

carbon bed. Fig. 8 shows the curves obtained for PS at different feed concentrations and the pH profiles.

The dynamic behavior of a fixed bed column is described in terms of the concentration-time profile of the effluent, called rupture curve. The shape of this curve is determined by the shape of the equilibrium isotherm and influenced by the individual transport processes in the column. Several mathematical models for the prediction of the dynamic behavior of the column have been developed. Among them, Thomas and dose response models are the most frequently used, and are applied in this work to estimate and analyze the adsorption performance in the column. The parameters obtained for each model for lead adsorption at 25 and 100 mg L^{-1} using samples PS, PL, CS and CL are presented in Tables 5 and 6. The regression coefficient (R^2) and the RMSE are also informed as estimators of the goodness of fit of the models.

The values of the regression coefficient (R^2) indicate the Thomas model closely matches the empirical data of the column for lead adsorption (0.913–0.998). It is observed that the change in the initial metal ion concentration has a significant effect on the breakthrough curve. The rate constant (k) of the Thomas model decreased with the increase in the initial input concentration, attributed to a greater resistance in mass transport, while the adsorption capacity (q) grew according to the values estimated by both models. A higher feed concentration, which is reflected in a greater driving force for mass transfer, leads to a decrease in the length of the adsorption zone. The net impact is an increase in the adsorption capacity [33].

Breakthrough curves show a greater deviation related to experimental data for Thomas model, than for Dose Response Model. These differences are more important at very small and very large operation times, when the concentration-time profile does not present the typical sigmoidal shape. The modified dose response model describes the entire rupture curve with a better fit to the experimental data, the goodness of fit is reflected in the higher values of the correlation coefficient ($0.967 \leq R^2 \leq 0.999$) and in the lower values of RMSE. It overcomes an important inconsistency of Thomas model that assigns a fixed normalized output concentration when

Table 5
Thomas model parameters

Initial concentration: C_0 (mg L^{-1})	Parameter	PS	PL	CS	CL
25	k (L (mg min)$^{-1}$)	9.1×10^{-5}	5.4×10^{-4}	1.1×10^{-4}	4.9×10^{-4}
	q (mg g^{-1})	39.24	48.62	11.39	3.09
	R^2	0.986	0.998	0.967	0.985
	RMSE	1.18	0.50	1.60	0.93
	k (L (mg min)$^{-1}$)	8.9×10^{-5}	7.3×10^{-5}	9.1×10^{-5}	1.9×10^{-4}
100	q (mg g^{-1})	40.14	49.10	14.50	5.09
	R^2	0.998	0.978	0.913	0.951
	RMSE	2.16	6.27	12.13	6.92

Table 6
Dose response model parameters

Initial concentration: C_0 (mg L^{-1})	Parameter	PS	PL	CS	CL
25	a	7.48	53.9	2.23	2.26
	q (mg g^{-1})	38.74	47.38	10.08	2.7
	R^2	0.999	0.998	0.992	0.994
	RMSE	1.03	0.49	0.82	0.60
	a	8.07	10.66	2.19	1.75
100	q (mg g^{-1})	39.30	48.30	13.27	4.25
	R^2	0.997	0.981	0.967	0.985
	RMSE	2.64	5.71	7.48	3.82

the experimental time or volume is zero, which is contrary to real conditions [22].

Table 7 presents the breakthrough (t_b) and the exhaustion time (t_e) for the adsorption assays performed with the activated carbon samples at 100 and 25 mg L^{-1} concentrations. As feed concentration increased, these parameters decreased for all the adsorbents. These results demonstrate that the change of concentration gradient affects the saturation rate and breakthrough time, or in other words, the diffusion process is concentration dependent.

In Table 7, it is also informed the parameter q_{10}, which is the mass of the contaminant retained in the solid at the breakthrough point, and can be calculated as follows:

$$q_{10} = \frac{Q_v t_b C_0}{1{,}000\, m} \tag{10}$$

where t_b is the breakthrough time (min), Q_v is the volumetric feed flow (cm^3 min^{-1}), C_0 is the concentration of the incoming solution (mg L^{-1}) and m is the mass of adsorbent (g) [30].

The maximum adsorption capacity was 49.10 mg g^{-1}, achieved at a bed height of 15 cm and a feed concentration of 100 mg L^{-1} using grape lex briquettes activated with steam as adsorbent. This result shows a significant reduction in the adsorption capacity of the column experiments compared with that reported from the adsorption isotherm. The difference found when the removal process is performed in batch mode can be justified considering that in the first, activated carbon is in constantly stirred and moves freely, allowing a complete mixing and providing a better interaction between active sites of the adsorbent and Pb(II) ions. In addition, activated carbon remains longer in contact with the solution allowing to reach the equilibrium conditions. Both situations favor the mass transfer and thus the retention of lead ions. The differences between the results obtained for static and continuous tests could be reduced working at lower volumetric feed flows, which increase the column residence time. There are some limitations for this reduction because low feed rates could lead to by passes in the packed bed.

Regeneration of the adsorbent material is a very important feature in the economic development. The aim is to remove the loaded metal from the column in the smallest possible volume of an eluting solution. The ideal regeneration process should produce small volume of metal concentrates suitable for metal-recovery without adsorption capacity depletion, making it reusable in several adsorptions and desorption cycles.

In this work, desorption tests were performed to evaluate bed regeneration by elution with nitric acid under the same conditions of adsorption tests. The effectiveness of metal desorption was calculated through the ratio of metal eluted in desorption tests to metal retained in the solid during the adsorption tests.

The concentration of lead that remains unbound at equilibrium (C_e) corresponds to the area under the breakthrough curve, and can be defined as:

$$C_e = \frac{(m_T - m_E)}{V_E} \tag{11}$$

where m_T is total amount of lead ions sent to the column (mg), m_E is total amount of lead ions bound in a fixed bed of adsorbent (mg) and V_E is effluent volume at the point of exhaustion (L).

The total quantity of lead ions bound in a fixed bed of adsorbent for a given feed concentration and flow rate through the column was determined by integration of the area above the breakthrough curve, and can be calculated according to the equation:

$$m_E = Q\int_0^{t_E} (C_0 - C)\mathrm{d}t \tag{12}$$

Table 7
Parameters for lead adsorption in column by activated carbons obtained from lex and stalk grape

Initial concentration: C_0 (mg L^{-1})	Parameter	PS	PL	CS	CL
100	t_r (min)	550	850	75	90
	t_a (min)	1,120	1,550	200	250
	m_a (g)	6.3	8.7	3.4	6
	Q_v (mL min^{-1})	3.1	4.3	1.7	3
	q_{10} (mg g^{-1})	27.06	42.01	3.75	4.57
25	t_r (min)	2,600	3,850	410	100
	t_a (min)	4,350	4,250	1,610	300
	m_a (g)	6.1	8.6	3.5	5.9
	Q_v (mL min^{-1})	3.1	4.3	1.7	3
	q_{10} (mg g^{-1})	33.03	48.13	5.13	1.27

where C_0 is the initial concentration of lead (mg L^{-1}), C is the concentration of lead in the effluent, (mg L^{-1}), Q is the flow rate (L s^{-1}), t is the time (s) and t_E is the time necessary to reach the exhaustion point of the adsorbent bed (s).

The amount of metal retained in the adsorption tests and the total amount of adsorbate eluted in desorption tests were determined using the method of Newton for graphical integration:

$$m_{\text{metal}} = \frac{(\mathrm{d}V \times C_{\text{average}})}{\text{mass}_{\text{adsorbent}}} \tag{13}$$

where m_{metal} is expressed in mg g^{-1}, dV in L and C_{average} in mg L^{-1}. The value of dV is calculated as the difference in volume between two time points. The C_{average} value in mg L^{-1} is calculated as the average concentration retained or desorbed ($C_{\text{solid},i}$) between two instants of time, as expressed in the following equation:

$$C_{\text{average}} = \frac{(C_{\text{solid},i} + C_{\text{solid},i-1})}{2} \tag{14}$$

The total metal concentration on the adsorbent (C_{solid}) corresponds to the difference between the initial concentration of the solution at the inlet of the column and its value at the output.

$$C_{\text{solid}} = C_0 - C_{\text{output}} \tag{15}$$

Desorption yield was evaluated by the ratio of desorbed metal retained on the solid during the test. For all the adsorbents, under the same operating conditions, the average efficiency of washing was around 78%.

Fig. 9 shows elution profiles for the studied activated carbons at the different initial concentrations tested in continuous assays. It can be observed that all adsorbents showed similar behavior in elution assays. A high concentration peak appears when 50 mL of eluent is passed through the column,

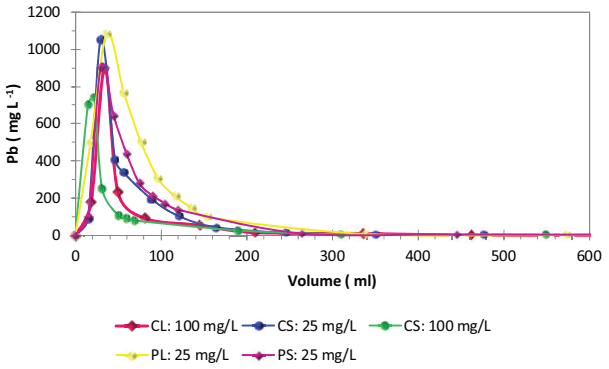

Fig. 9. Elution profile for physically and chemically activated carbons at eluent concentration of 0.5 mg L^{-1}. Conditions: bed height = 150 mm, T = 293 K and HNO_3 as eluent.

which corresponds to the first 30 min of operation. It can be observed that there is no important demand of eluent and time. The result is low volumes of solution with a high metal concentration which enables its recovery for other uses. This is an indicative of the facility of regeneration, a desirable feature of any adsorbent.

4. Conclusions

Physical and chemical activation methods of grape stalk and lex produced adsorbents with good textural properties. All adsorbents showed similar micropore volume, but chemically activated carbons had higher mesopore volumes and also higher surface areas. Physically activated carbons showed pH_{pzc} markedly high, revealing the basic character of these carbons. Chemical adsorbents had higher content of surface functional groups.

The performance of the chemically activated carbons in batch assays was better, reaching removals that exceed 100 mg g^{-1} for both materials. These results indicated that the porous development and the oxygen surface groups present in the adsorbent surfaces were combined favorably for metal retention.

The results of the tests performed in fixed bed columns revealed that the adsorbents derived from stalk and grape lex can be used for the removal of Pb(II) ions from aqueous solution in continuous operation. The highest adsorption capacity, corresponding to grape lex physically activated, was around 50 mg g^{-1}. The behavior of the activated carbons was markedly influenced by adsorbents pH_{pzc}, so lead removal was related with the confluence of adsorption and precipitation phenomena. The experimental breakthrough curves were properly described by Thomas and modified dose response models, a good agreement between the predicted and experimental breakthrough values was observed. Sorption parameters, obtained by both models, were influenced by the inlet lead(II) ion concentration. At the highest Pb(II) concentration, the column saturated more quickly, leading to lower breakthrough and exhaustion times.

References

[1] M. Prado Cechinel, M. Guelli Ulson de Souza, A. Ulson de Souza, Study of lead (II) adsorption onto activated carbon originating from cow bone, J. Cleaner Prod., 65 (2015) 342–349.

[2] G. Issabayeva, M. Kheireddine Aroua, N. Meriam Sulaiman, Study on palm shell activated carbon adsorption capacity to remove copper ions from aqueous solutions, Desalination, 262 (2010) 94–98.

[3] R. Bansal, J. Donnet, F. Stoeckli, Active Carbon, Marcel Dekker Inc., New York, 1988.

[4] J.T. Nwabanne, P.K. Igbokwe, Adsorption performance of packed bed column for the removal of lead (II) using oil palm fibre, Int. J. Appl. Sci. Technol., 2 (2012) 106–115.

[5] S. Álvarez Torrellas, R. García Lovera, N. Escalona, C. Sepúlveda, J.L. Sotelo, J. García, Chemical-activated carbons from peach stones for the adsorption of emerging contaminants in aqueous solutions, Chem. Eng. J., 279 (2015) 788–798.

[6] M.T. Izquierdo, A. Martínez de Yuso, B. Rubio, R. Pino, Conversion of almond shell to activated carbons: methodical study of the chemical activation based on an experimental design and relationship with their characteristics, Biomass Bioenergy, 35 (2011) 1235–1244.

[7] R. Baccara, J. Bouzida, M. Fekib, A. Montiela, Preparation of activated carbon from Tunisian olive-waste cakes and its application for adsorption of heavy metal ions, J. Hazard. Mater., 162 (2009) 1522–1529.

[8] M.F. Sardella, M. Gimenez, C. Navas, C. Morandi, C. Deiana, K. Sapag, Conversion of viticultural industry wastes into activated carbons for removal of lead and cadmium, J. Environ. Chem. Eng., 3 (2015) 253–260.

[9] L. Oliveira, E. Pereira, J.R. Guimaraes, A. Vallone, M. Pereira, J. Mesquita, K. Sapag, Preparation of activated carbons from coffee husks utilizing $FeCl_3$ and $ZnCl_2$ as activating agents, J. Hazard. Mater., 65 (2009) 87–94.

[10] C. Deiana, F. Sardella, H. Silva, A. Amaya, N. Tancredi, Use of grape stalk, a waste of the viticulture industry, to obtain activated carbon, J. Hazard. Mater., 172 (2009) 13–19.

[11] F.J. García-Mateos, R. Ruiz-Rosas, M.D. Marqués, L.M. Cotoruelo, J. Rodríguez-Mirasol, T. Cordero, Removal of paracetamol on biomass-derived activated carbon: modeling the fixed bed breakthrough curves using batch adsorption experiments, Chem. Eng. J., 279 (2015) 18–30.

[12] ASTM D 2866-94 ASTM Committee on Standards, 1916 Race St., Philadelphia, PA, 1994, p. 727.

[13] ASTM D 2867-95 ASTM Committee on Standards, 1916 Race St., Philadelphia, PA, 1995, p. 729.

[14] ASTM E 872-98 ASTM Committee on Standards, 100 Barr Harbor Drive, West Conshohocken, PA, 1998, p. 270.

[15] J. Noh, J. Schwartz, Estimation of the point of zero charge of simple oxides by mass titration, J. Colloid Interface Sci., 3 (1989) 157–164.

[16] A.C. Deiana, M. Gimenez, S. Rómoli, M.F. Sardella, K. Sapag, Batch and column studies for the removal of lead from aqueous solutions using activated carbons from viticultural industry wastes, Adsorpt. Sci. Technol., 32 (2014) 181–195.

[17] S. Lagergren, Zur theorie der sogenannten adsorption geloster stoffe, K. Sven. Vetensk.akad. Handl., 24 (1898) 1–39.

[18] Y.S. Ho, G. Mckay, The sorption of lead(II) on peat, Water Res., 33 (1999) 578–584.

[19] H. Freundlich, About the adsorption in solutions, Z. Phys. Chem., 57 (1906) 385–470.

[20] I. Langmuir, The adsorption of gases on plane surfaces of glass, mica and platinum, J. Am. Chem. Soc., 40 (1918) 1361–1403.

[21] Z. Xu, J. Cai, B. Pan, Mathematically modeling fixed-bed adsorption in aqueous systems, J. Zhejiang Univ. Sci. A (Appl. Phys. Eng.), 14 (2013) 155–176.

[22] G. Yan, T. Viraraghava, M. Chen, A new model for heavy metal removal in a biosorption column, Adsorpt. Sci. Technol., 19 (2001) 25–43.

[23] K. Johari, A. Alias, N. Saman, S. Song, Removal performance of elemental mercury by low-cost adsorbents prepared through facile methods of carbonization and activation of coconut husk, Waste Manage. Res., 33 (2015) 81–88.

[24] P. Brende, R. Gadiou, J.-C. Rietsch, P. Fioux, J. Dentzer, A. Ponche, C. Vix-Guterl, Characterization of carbon surface chemistry by combined temperature programmed desorption with in situ X-ray photoelectron spectrometry and temperature programmed desorption with mass spectrometry analysis, Anal. Chem., 84 (2012) 2147−2153.

[25] J.L. Figueiredo, M.F.R. Pereira, The role of surface chemistry in catalysis with carbons, Catal. Today, 150 (2010) 2–7.

[26] L. Giraldo, J.C. Moreno-Piraján, Pb^{2+} adsorption from aqueous solutions on activated carbons obtained from lignocellulosic residues, Braz. J. Chem. Eng., 25 (2008) 143–148.

[27] W. Tongpoothorn, M. Sriuttha, P. Homchan, S. Chanthai, C. Ruangviriyachai, Preparation of activated carbon derived from *Jatropha curcas* shell by simple thermo-chemical activation and characterization of their physico-chemical properties, Chem. Eng. Res. Des., 8 (2011) 335–340.

[28] B. Aceved, C. Barriocanal, Texture and surface chemistry of activated carbons obtained from tyre wastes, Fuel Process. Technol., 134 (2015) 275–283.

[29] A. Puziy, O. Poddubnaya, A. Martinez-Alonso, F. Suarez-García, J. Tascón, Surface chemistry of phosphorus-containing carbons of lignocellulosic origin, Carbon, 43 (2005) 2857–2868.

[30] M. Machida, T. Mochimaru, H. Tatsumoto, Lead(II) adsorption onto graphene layer of carbonaceous materials in aqueous solution, Carbon, 44 (2006) 2681–2688.

[31] M. Abbas, S. Kaddourb, M. Trari, Kinetic and equilibrium studies of cobalt adsorption on apricot stone activated carbon, J. Ind. Eng. Chem., 20 (2014) 745–751.

[32] F. Wu, R. Tseng, S. Huang, R. Juang, Characteristics of pseudo-second-order kinetic model for liquid-phase adsorption: a mini-review, Chem. Eng. J., 151 (2009) 1–9.

[33] J. Goel, K. Kadirvelu, C. Rajagopal, V.K. Garg, Removal of lead(II) by adsorption using treated granular activated carbon: batch and column studies, J. Hazard. Mater., 125 (2005) 211–220.

[34] G.C. Castellar Ortega, Master's Thesis: Remoción de Pb (II) en disolución acuosa sobre carbón activado: Experimentos en columna, Convenio de cooperación Universidad Nacional de Colombia–Universidad del Magdalena, Bogotá D.C., Colombia, 2012.

[35] C. Faur-Brasquet, Z. Reddad, K. Kadirvelu, P. Le Cloirec, Modeling the adsorption of metal ions (Cu^{2+}, Ni^{2+}, Pb^{2+}) onto ACCs using surface complexation models, Appl. Surf. Sci., 196 (2002) 356–365.